

AVOIDING MICRO-PRESSURE WAVES WITHOUT BUILDING TUNNEL HOODS

¹Feng LIU, ²Dubravka POKRAJAC, ³Alan VARDY

¹*College of Mechanical and Vehicle Engineering, Taiyuan University of Technology, China*

²*School of Engineering, University of Aberdeen, UK*

³*University of Dundee and Dundee Tunnel Research, UK*

ABSTRACT

The use of arrays of air-storage chambers to prevent unacceptable MPWs radiating from tunnels is investigated. Geometrically, the chambers are closely similar to Helmholtz resonators that have been assessed by previous researchers. However, the connections between the chambers and the tunnel have sufficiently high resistance to prevent oscillations that Helmholtz resonators are designed to encourage. The effectiveness of the air-storage chambers is found to depend not only on their key properties (volume and resistance), but also on the initial properties of the wavefront (amplitude, steepness) - e.g. at train nose-entry to a tunnel. It is found that the use of such chambers could be effective and hence that they are a plausible alternative to providing long hoods at tunnel entrances. However, practical issues remain to be assessed in detail, notably regarding potential maintenance requirements.

Keywords: Air-storage chambers, micro-pressure waves, wavefront steepening, Helmholtz resonators, asymptotic wavefronts

1. INTRODUCTION

It is well known that when the pressure waves generated by trains in tunnels reach an exit portal, pressure disturbances radiate into the surrounding environment. When the waves are sufficiently steep, the radiated micro-pressure waves (MPWs) can be unacceptably large and so remedial action is required. In principle, this can be met by special features at the tunnel exit (Howe & Cox 2005, Wang et al 2015), but in practice, the chosen solution is to ensure that the waves arriving at the exit are sufficiently gentle for nuisance to be avoided. The most common method of achieving this is by constructing a hood at the tunnel entrance to ensure that train-entry does not generate waves that are too steep (Howe 1999, Miyachi et al 2015).

The required length of a tunnel entrance hood increases with increasing train speed and with decreasing tunnel cross-sectional areas. As a consequence, recent proposals have included designs for hoods exceeding over 100 m (Sturt et al 2015). These can be costly (construction and land-take) and it can be challenging to achieve visually acceptable solutions. Also, it is not always practicable to propose the use of long hoods – e.g. when the portals are in densely populated areas or in other constrained locations – see Fig-1, for instance. A further limitation is that, at least in principle, it is possible for trains to generate significant waves during travel through tunnels. Such waves are wholly uninfluenced by entrance portals. To date, this issue has not been a major concern, partly because it can be addressed locally within the tunnel. Even so, it would not be safe to completely ignore it during design.

It would clearly be desirable to have a remedial measure that avoids the need for any special features at tunnel portals. Ideally, a one-solution-fits-all design within the tunnel itself should be found. This is not an unrealistic aspiration. After all, tunnels with ballast track are much less susceptible to creating MPWs than tunnels with slab track. Indeed, it is rare (perhaps unknown?) for significant MPWs to be emitted from *long* ballast track tunnels. The reasons for this are not

fully understood, but enough is known to enable designs to be undertaken with a reasonable degree of confidence. Unfortunately, ballast track has important disadvantages, notably the need for regular maintenance and the risk of individual stones becoming projectiles when air speeds are high. As a consequence, slab track is increasingly preferred for high-speed operation and so remedial measures are needed to prevent MPWs.

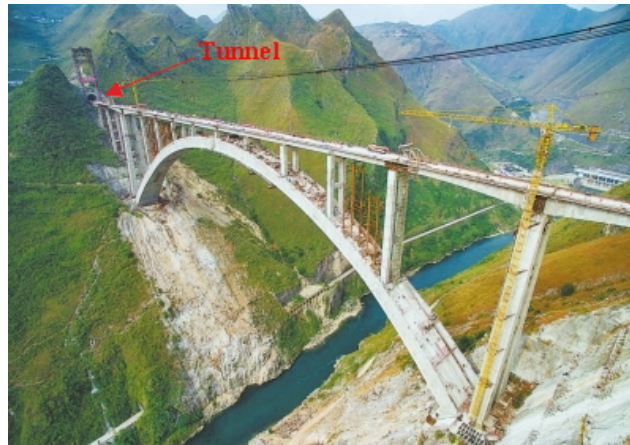


Figure 1: Beipanjiang bridge in southwest China (*Li et al., 2019*)

This paper proposes such a method. It was inspired by research by Vardy & Brown (2000) on wave propagation in ballast track tunnels. The analysis that they used fell short of providing a full description of the influence of ballast, but it did predict similar overall behaviour. Its greatest limitation was an inability to relate ballast properties (porosity, stone size distribution) directly to coefficients used in the analysis. After writing that paper, the authors realised that direct advantage could be taken of the similarity because it should be possible to construct bespoke conditions that approximate to the theoretical model more closely than ballast itself. The present paper presents a simple geometry that achieves this objective and is well-suited to use in slab-track tunnels.

2. AIR STORAGE CHAMBERS

Figure-2 is a schematic representation of the proposed method. Air-storage chambers are created over long distances, perhaps even over the whole length of the tunnel in some cases. In the figure, they are depicted as spherical, but this is for illustrative purposes only. Within wide limits, their shape has negligible influence on their influence. Their most important properties are (i) their volume and (ii) the resistance to airflows between them and the main tunnel cross-section. Also, it is important that they are not connected to one another; that is, air must not be allowed to flow from one chamber to the next.

The figure depicts a wavefront propagating along a region of tunnel with air-storage chambers. When the leading edge of the wavefront reaches any particular chamber, air begins to flow into the chamber. This process then continues until the maximum pressure in the wavefront arrives. Eventually, other waves will cause a decrease in pressure and air will flow out of the chamber. However, this is not relevant of the main purpose, namely preventing steepening of compressive wavefronts and, ideally, even reducing their steepness. The sketch illustrates schematically how the steepness of a wavefront might evolve as it propagates along a tunnel. In this instance, the depicted evolution illustrates gradually reducing steepness. This contrasts with gradually increasing steepness that is typical in conventional slab-track tunnels. At any instant, the steepness varies along the wavefront, being small at the toe and heel and a maximum at some

mid-point. For MPW purposes, the maximum steepness is the key parameter because this is the dominant factor influencing the strength of radiated MPWs. In this paper, the maximum steepness is used as the key characteristic of wavefronts when assessing the influence of air-storage chambers.

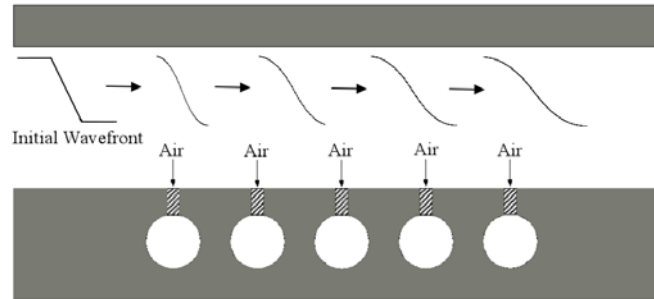


Figure 2: Schematic diagram showing air-storage chambers

Attention is drawn to two important aspects of this process:

- (i) the storage capacity of the chambers is a function of the increase in density and this automatically increases as the wavefront pressure increases;
- (ii) the effectiveness of the chambers for wave attenuation is critically dependent on the resistance to flow from the tunnel into the chambers. If the resistance is too small, the changes in pressure in the chambers will be almost in phase with those in the tunnel. If it is too large, the changes in the chambers will lag too much behind the tunnel pressures. In that case, they would not exert maximum effect where it is needed, namely in the most rapidly changing period as the wavefront passes by.

These considerations are explored in more detail below.

At first sight, the proposed air-storage chambers could be mistaken for an array of Helmholtz resonators. Indeed, in a strict academic sense, that is what they are. However, there is a crucial difference from more usual Helmholtz resonators (e.g. Sugimoto 1992, Tebbutt et al 2017), namely that the connections between the tunnel and the chamber are expressly required to prevent resonance. In the proposed design, the inertance of the connections has negligible influence on rates of airflow through them. Instead, the chosen resistance is so large that, for practical purposes, it may be regarded as the only controlling factor.

3. THEORETICAL METHODOLOGY

The theoretical methodology used in this work closely mirrors that presented by Vardy & Brown (2000) so it is not presented in detail herein. Instead, key features are highlighted and attention is drawn to differences. In both cases, the analysis is based on the one-dimensional (1-D) Method of Characteristics (MOC) and the solution sequence takes advantage of the fact that the primary direction of wave propagation is known a-priori. Small reflected waves generated at each air chamber travel in the opposite direction to the main wavefront, but these are very much smaller than the main wavefront. Accordingly, the numerical grid can be matched to the speed of wave propagation, thereby greatly reducing numerical interpolations that cause non-physical dispersion of waves in more general uses of MOC. The connections between the tunnel and the air chambers are located at grid points, not distributed continuously along the tunnel. However, this is unimportant because the grid spacing is much smaller than a tunnel diameter.

In all results presented herein, the air chambers are modelled as discrete volumes in which conditions are spatially uniform even though they vary in time. This is justified because their dimensions are much smaller than a tunnel diameter. Flows between them and the tunnel are

simulated as quasi-steady and regarded as being driven by the difference between the bulk pressure in a chamber and the average pressure in the adjacent tunnel cross-section. In common with Vardy & Brown (2000), it is assumed that resistance to flow through the connections is proportional to the velocity of flow. To achieve this, the most likely configuration of the connections will be numerous small-bore passages (i.e. a porous barrier of some sort). One particular possibility is presented below, but the analysis is applicable to any configuration that behaves linearly. The authors have also studied connections that behave in a quadratic manner and have obtained broadly similar outcomes. However, the quadratic connections are found to be less effective than linear ones so, for brevity, they are not considered further herein.

Unlike the analysis presented by Vardy & Brown, no allowance is made for the influence of inertia on flows through the connections. Numerically, this is an especially helpful simplification because it reduces potential causes of instability. However, it also prevents the use of the analysis for cases where the inertia has a significant influence. As a check on this matter, Figure-3 compares predictions from the current method with those presented by Vardy & Brown. It shows how wavefronts of different initial steepness evolve as they propagate along the tunnel. For this particular figure, the various dimensions and properties are necessarily those used in the earlier paper. Inevitably, small differences exist, but the close agreement between the two methods gives confidence in both analyses. Herein, a third-order predictor-corrector method has been used. It is believed that a first-order method was used in the earlier paper although this is not recorded in the paper.

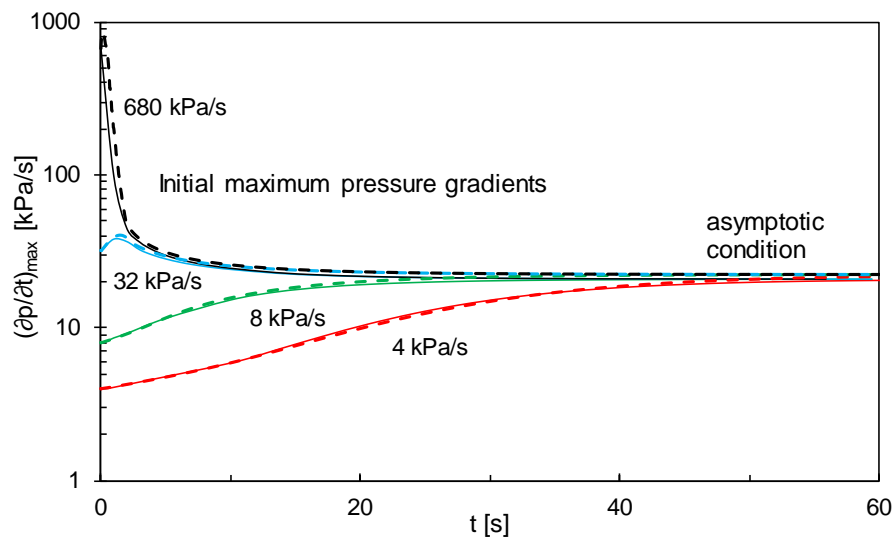


Figure 3: Comparison of current methodology (broken lines) with Vardy & Brown (2000) (continuous lines)

4. ASYMPTOTIC WAVEFRONT

An important feature of Fig-3 above is that all four curves converge towards a common asymptote. That is, after propagating sufficiently far, the wavefront shape is no longer dependent upon the initial shape. Instead, for any particular wavefront amplitude, the wavefront shape evolves to one that is determined solely by the air-storage chambers. This is true regardless of whether the initial wavefront is more-steep or less-steep than the asymptotic state. At first sight, this prediction can be counter-intuitive because it differs so strongly from known behaviour in slab-track tunnels. However, it is broadly equivalent to behaviour measured in ballast-track tunnels so it is entirely reasonable. In fact, wavefronts in some ballast track tunnels have been observed to steepen initially and then to continually reduce in steepness – in the

manner shown in Fig3 for the wavefront with an initial steepness of 32 kPa/s. In practice, the rates of change of maximum steepness are influenced by skin friction as well as by ballast (or by air chambers), but this effect is neglected herein.

Given this general behaviour, two questions arise, namely (i) “how does the asymptotic shape of the wavefront depend on the properties of the air-storage chambers?” and (ii) “how far must the wavefront travel before it approaches the asymptote?” The first of these questions is addressed in this Section and the second is considered in Section 5. The shape of the chosen initial wavefront (Fig-4) is one used by Wang et al (2018). It is of finite length and its simple ‘S’ shape is loosely indicative of train-entry wavefronts. It is preferred to the commonly chosen arctan shape because that is asymptotic at its leading and trailing edges and therefore necessitates arbitrary numerical adjustment in computer simulations.

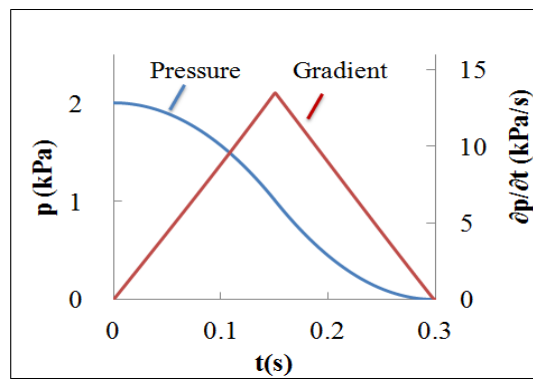


Figure 4: Prescribed initial wavefront shape

Several independent parameters influence the shape of the resulting asymptotic wavefront. It would not be practicable (or helpful) to present a full parametric study herein so, instead, a sensitivity study is centred on a specific base case. The base case is defined in Table-1 and the sensitivity study is presented in Fig-5. In each box in Fig-5, the values of all parameters except one are the same as in the base case.

Figure-5(a) shows the influence of the volumetric ratio of the chambers and the tunnel, namely the ratio of the total volume of all chambers in a given length of tunnel to the total volume of air in the same length of tunnel. As would be expected, very small ratios have relatively little influence whereas larger ratios have successively greater influence. The upper limit to the range shown is determined by practical considerations, not by theoretical limitations. It should be noted that the trend shown in the figure is applicable when the same resistance coefficient is used in all cases. In practice, the chosen value has been optimised for the base case. It is likely that a full parametric study would show some dependence of the optimum value on the volume ratio.

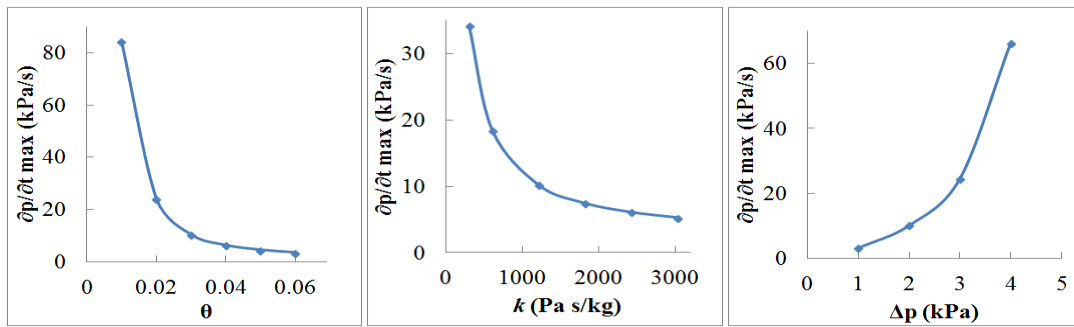
Figure-5(b) shows the influence of the resistance coefficient for flow through the connectors. By inspection, an optimum value exists. Smaller values enable too much air to enter the chambers near the toe of the wavefront and hence reduce the capacity available for attacking the more important steeper parts of the wavefront. Larger resistances yield smaller maximum gradients, but they do so only after travelling large distances. To avoid presenting results that would imply excessively long tunnels, the ‘asymptotic’ conditions shown in the Figure are conditions after the wavefront has travelled 12 km.

Table 1: Specification of base case values

Parameter	Value	Notes
Tunnel		
Cross-sectional area	100 m ²	This is a nominal size. The chamber:tunnel volume ratio is more important than the absolute values
Friction coefficient	0	Skin friction would be included in practical design, but it is a second-order effect. Its inclusion herein would mask the influence of air-storage chambers
Air-storage chambers		
Chamber:tunnel volume ratio	3%	This proportion might be readily achievable in many tunnels. Larger values are preferable
Connector resistance	1200 Pa.s/kg	Assumes linear resistance - e.g. a pressure difference of 1.2 kPa causes a flow rate of 1 kg/s
Wavefront		
Amplitude	2 kPa	
Initial length	100 m	Typical of nose-entry wavefronts on high-speed lines
Initial $(\partial p / \partial t)_{\max}$	13.2 kPa/s	<i>(based on a sound speed of 330 m/s)</i>
Numerical grid		
Spatial step (Δx)	0.250 m 0.125 m	For asymptotic wavefront calculations For wavefront evolution calculations <i>(Demonstrated to give good numerical accuracy)</i>
Temporal step (Δt)	$\Delta x / U_{\text{wave}}$	Time required for the mid-point of wavefront to travel a distance Δx

Figure 5(c) shows the influence of the wavefront amplitude. It shows that, for fixed values of the volume ratio and the resistance coefficient, the maximum gradient increases strongly with the wavefront amplitude. Furthermore, the dependence is strongly non-linear, being strongest at large amplitudes that are increasingly likely to exist as train speeds increase and tunnel cross-sections are constrained on cost grounds.

Overall, Fig-5 indicates that the effectiveness of the air-storage chambers will depend quite strongly on their design. However, in any particular instance, the tunnel dimensions and the maximum train speed will be known a-priori – so choosing the most suitable properties of the chambers will be feasible on a case-by-case basis.



(a) Chamber:tunnel volume ratio (b) Connector resistance (c) Wavefront amplitude

Figure 5: Influence of key parameters on the asymptotic wavefront

5. EVOLUTION OF WAVEFRONTS

Although the asymptotic wavefront condition is important for general understanding, it is not sufficient information for design purposes. As Fig-3 above shows, the time taken to approach the asymptotic state closely can be quite large. As a numerical example, suppose that the time required in a particular case is 10 seconds. In this time, the wave will have travelled along approximately 3½ km of tunnel, all of which must have air-storage chambers. From this, we can make two significant inferences, one ‘good’ and one ‘bad’. The good news is that, regardless of the overall length of the tunnel, only 3½ km of it would need to have air-storage chambers. This region must, however, be adjacent to the exit portal – because wavefronts will recommence their usual steepening after leaving a region with air-chambers. The bad news is that the chosen air-chambers would not lead to an asymptotic state in a tunnel that is shorter than 3½ km – although a different configuration might do so.

It is evident that attention must be paid to the evolving shapes of wavefronts as they propagate along a tunnel. In this respect, a further useful deduction from Fig-3 is that wavefronts that are initially steeper than the asymptotic state tend to be influenced more rapidly than wavefronts that are initially less steep. This supports the above suggestion of having the chambers only in the region upstream of an exit portal. In this case, the wavefront would steepen normally until reaching the chambers and would then rapidly reduce in steepness before reaching the portal.

Figure-6 shows the dependence of the evolution of the maximum wavefront steepness on the principal parameters. The horizontal axis is shown as the distance travelled by the wavefront. For design purposes, this is more informative than the time of travel.

Figure-6(a) illustrates the influence of the chamber:tunnel volume ratio. By inspection, not only does the asymptotic steepness reduce with increasing chamber volume (Fig-5(a)), but also the rate at which it approached the asymptote increases. This is an expected result because larger chambers can remove larger amounts of air from the wavefront. Figure-6(b) illustrates the influence of the resistance of the connectors. The figure is quite instructive because it shows that the relative effectiveness of different resistances depends upon the length of tunnel over which they are distributed. Figure-6(c) illustrates the importance of the wavefront amplitude (and hence the train speed). The base-case chambers prevent steepening of the 2 kPa wavefront, but the stronger wavefronts continue to steepen throughout the simulated length of 5 km – even though their initial lengths have been increased to give the same maximum initial gradient in each case. Figure-6(d) illustrates the influence of the initial length of wavefronts of equal amplitude. This parameter was not considered in Fig-5 because it has no influence on the (true) asymptotic state. The figure confirms the trends already discussed for different system parameters in relation to Fig-3.

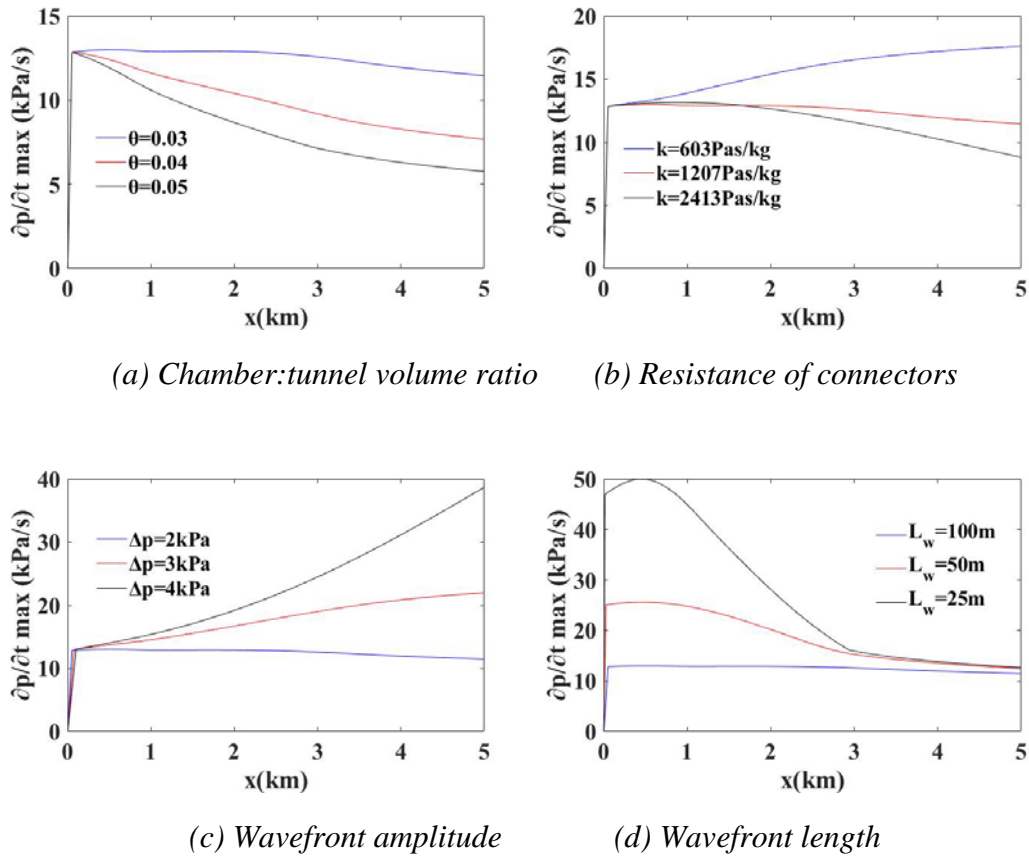


Figure 6: Influence of key parameters on the wavefront evolution

Figure-6(a) illustrates the influence of the chamber:tunnel volume ratio. By inspection, not only does the asymptotic steepness reduce with increasing chamber volume (Fig-5(a)), but also the rate at which it approached the asymptote increases. This is an expected result because larger chambers can remove larger amounts of air from the wavefront. Figure-6(b) illustrates the influence of the resistance of the connectors. The figure is quite instructive because it shows that the relative effectiveness of different resistances depends upon the length of tunnel over which they are distributed. Figure-6(c) illustrates the importance of the wavefront amplitude (and hence the train speed). The base-case chambers prevent steepening of the 2 kPa wavefront, but the stronger wavefronts continue to steepen throughout the simulated length of 5 km – even though their initial lengths have been increased to give the same maximum initial gradient in each case. Figure-6(d) illustrates the influence of the initial length of wavefronts of equal amplitude. This parameter was not considered in Fig-5 because it has no influence on the (true) asymptotic state. The figure confirms the trends already discussed for different system parameters in relation to Fig-3.

6. PRACTICAL IMPLEMENTATION

So far, the discussion has focussed dominantly on theoretical predictions. However, having established that the method has strong potential in theory, it is appropriate to give initial consideration to more practical matters. Important issues include:

- Q1:** how can space be made available in the tunnel cross-section at reasonable cost?
- Q2:** can the connections between the tunnel and the air-storage chambers be created in a straightforward manner?
- Q3:** will the system require regular maintenance?

The first of these questions will be, to some extent, tunnel-dependent. For instance, many tunnels have walkways beneath which space is likely to be available. This space, together with space between and beneath the tracks might be available at little cost. Similarly, many tunnels are bored and space could be allocated on their sides, albeit detracting from the overall free-area in the cross-section and hence causing increased wavefront amplitudes. If these measures are insufficient, it will be necessary to increase the overall cross-section of the tunnel to accommodate the additional required size. This has obvious cost implications and it is impractical in already-built tunnels.

The second question is easier to answer. The total surface area between the chambers and the main tunnel is likely to be large so a range of options will exist for creating the desired resistance. However, in all cases, the necessary resistance is high and so its provision will require multiple, very small passages/tubes/etc. Clearly, measures will need to be taken to prevent blockage by dust and other particulate matter. Otherwise, frequent maintenance could become necessary, thereby greatly reducing the desirability of the overall methodology. At this stage, the authors need to hide behind the argument that they are primarily presenting an apparently attractive idea that has been verified academically, but that has yet to be studied seriously as a practical proposition. Input from practising engineers with relevant experience would be most welcome.

7. CONCLUSIONS

The use of arrays of air-storage chambers to prevent unacceptable MPWs radiating from tunnels has been investigated. The connections between the chambers and the tunnel have sufficiently high resistance to ensure super-critical damping and hence prevent oscillations typical of Helmholtz resonators. Conclusions that can be drawn from the study include:

1. In the presence of such chambers, wavefronts evolve towards an asymptotic condition that depends on the volume of the chambers and the resistance of the connectors.
2. The asymptotic state depends upon the amplitude of the wavefront, but is independent of its upstream steepness, regardless of whether this is initially larger or smaller than the asymptotic state.
3. The time required to approach the asymptotic state can be large so practical design will need to include consideration of the evolution of wavefronts towards this state.
4. The evolution depends on the upstream steepness of the wavefront as well as upon its amplitude.
5. It has been shown that the chambers are, in principle, capable of being used to prevent MPWs, at least from long tunnels, provided that sufficient space is available in the tunnel cross-section.
6. Despite the positive outcome in principle, important practical matters still need to be addressed regarding the design of the connections between the tunnel and the chambers, especially in respect of potential issues related to maintenance.

ACKNOWLEDGEMENTS

The authors are grateful to the following bodies that provided financial support for the project: (a) China Scholarship Council (201806935055), (b) State Key Laboratory of Traction Power (grant no. TPL1904), (c) Scientific and Technological Innovation Programs of Higher Education Institutions in Shanxi (grant no. 2019L0251), (d) Natural Science Foundation of Shanxi Province, China (grant no. 201801D221224).

REFERENCES

- Howe MS (1999) On the compression wave generated when a high-speed train enters a tunnel with a flared portal, *J Fluids & Structures*, **13**, 481-498
- Howe MS & Cox EA (2005) Reflection and transmission of a compression wave at a tunnel portal, *J Fluids & Structures*, **20**, 1043-1056
- Li W, Liu T & Huo X (2019) Influence of the enlarged portal length on pressure waves in railway tunnels with cross-section expansion, *J Wind Engineering & Industrial Aerodynamics*, **190**, 10–22
- Miyachi T, Saito S, Fukuda T, Sakuma Y, Ozawa S, Arai T, Sakaue S & Nakamura S (2015) Propagation characteristics of tunnel compression waves with multiple peaks in the waveform of the pressure gradient (two papers), *J Rail & Rapid Transit*, **230(4)**, 1297-1317
- Sturt R, Baker CJB, Soper D, Vardy AE, Howard M & Rawlings C (2015) ‘The design of HS2 tunnel entrance hoods to prevent sonic booms’, *Proc 13th int conf on Railway Engineering, Edinburgh, UK, 30 June – 1 July 2015*
- Sugimoto N (2017) Propagation of nonlinear acoustic waves in a tunnel with an array of Helmholtz resonators, *J Fluid Mechanics*, **244**, 55-78
- Tebbutt JA, Vahdati M, Carolan D & Dear JP (2017) Numerical investigation on an array of Helmholtz resonators for the reduction of micro-pressure waves in modern and future high-speed rail tunnel systems, *J Sound & Vibration*, **400**, 606-625
- Vardy AE & Brown JMB (2000) Influence of ballast on wave steepening in tunnels, *J Sound & Vibration*, **238(4)**, 595-615
- Wang H, Lei B & Bi H (2018) Wavefront evolution of compression waves propagating in high speed railway tunnels, *J Sound and Vibration*, **431**, 105–121
- Wang H, Vardy AE & Pokrajac D (2015) Perforated exit regions for the reduction of micro-pressure waves from tunnels, *J Wind Engineering & Industrial Aerodynamics*, **146**, 139–149